Proceedings Paper:
Worley, R. orcid.org/0000-0002-3607-2650 and Anderson, S. (2020) Topological robot localization in a large-scale water pipe network. In: Mohammad, A., Dong, X. and Russo, M., (eds.) Towards Autonomous Robotic Systems 21st Annual Conference, TAROS 2020, Nottingham, UK, September 16, 2020, Proceedings. 21st Annual Conference, TAROS: Annual Conference Towards Autonomous Robotic Systems, 16 Sep 2020, Nottingham, UK. Lecture Notes in Computer Science, 12228 . , pp. 77-89. ISBN 9783030634858

https://doi.org/10.1007/978-3-030-63486-5_11

Topological Robot Localization in a Large-Scale Water Pipe Network

Rob Worley[0000−0002−3607−2650] and Sean Anderson ⋆

Department of Automatic Control and Systems Engineering, University of Sheffield, Sheffield, UK
rfworley1@sheffield.ac.uk

Abstract. Topological localization is well suited to robots operating in water pipe networks because the environment is well defined as a set of discrete connected places like junctions, customer connections, and access points. Topological methods are more computationally efficient than metric methods, which is important for robots operating in pipes as they will be small with limited computational power. A Hidden Markov Model (HMM) based localization method is presented here, with novel incorporation of measured distance travelled. Improvements to the method are presented which use a reduced definition of the robot state to improve computational efficiency and an alternative motion model where the probability of transitioning to each other state is uniform. Simulation in a large realistic map shows that the use of measured distance travelled improves the localization accuracy by around 70%, that the reduction of the state definition gives an reduction in computational requirement by 75% with only a small loss to accuracy dependant on the robot parameters, and that the alternative motion model gives a further improvement to accuracy.

Keywords: Topological Localization · Pipe Inspection Robots.

1 Introduction

Buried water pipe infrastructure is in regular need of maintenance, the cost of which may be reduced by more precisely locating faults. Robots could be used for autonomous, persistent monitoring of a pipe network. A principal challenge for this robotic system is to localize itself and faults in the network, and previous work on robot localization in pipes has used metric information from vision [1], inertial sensing [2] and acoustic sensing [3] [4]. However, while metric information is required for precise localization of a fault, localization to a single discrete pipe or junction would be sufficient for navigation and for isolating a fault to a part of the network.

A *topological* localization method for a single robot in a network of pipes is presented in this paper, where the robot is localized in a discrete set of places,

⋆ This work is supported by an EPSRC Doctoral Training Partnership Scholarship. S. Anderson acknowledges the support of EPSRC grant EP/S016813/1 (Pipebots)

the connection between which is described by a topological map. This is in contrast with *metric* localization methods, where a robot's location is described in a continuous space. The pipe environment is well defined by topological relations alone, as discrete places like junctions between pipes, customer connections, and above ground access points are connected together by pipes. Therefore, a topological method can be used in this application without the loss in precision that might be found when discretizing other environments into a topological map. In the pipe environment, typical metric methods have drawbacks. Methods that parameterise the robot state probability distribution, such as Kalman filtering and pose-graph optimization, poorly describe the multimodal probability distribution expected in a discrete network. Non-parameteric methods such as particle filtering have a higher computational cost, while a topological method would reduce the computation required for localization compared to metric methods, which is an advantage for robots with limited power and size which must operate in a typical pipe of 150mm diameter.

Early work in robot localization uses a topological map defined by distinctive places in a structured indoor environment [5] or segments between distinctive places [6]. Grid based maps can be divided into regions separated by narrow passages [7] or from a one-dimensional paths through the environment [8]. In much of this existing work, the focus is on obtaining a topological map from metric sensor data, which is less challenging in a pipe environment which is well described by only a topological map. However, the methods used in localization in the topological map are a useful foundation for this work.

A topological map representation has been shown to be useful in navigation where a Hidden Markov Model (HMM) localization method is extended to a Partially Observable Markov Decision Process (POMDP) [9]. Early work on localization in a pipe network [10] also uses a POMDP for localization and navigation, where the transition model between states is described, as is the observation model which finds the likelihood of an observation of the robot's surroundings at a junction corresponding to a known discrete type of junction.

Recent work on topological localization adds the challenges of erroneous repeated observations of the environment at a topological map node, inclusion of information assigned to nearby nodes, and failing to make an observation at a node [11], the last of which is especially applicable where a robot has limited sensing ability as is the case in a pipe environment. Use of geometric information on the robot's orientation has been applied using prior knowledge of the orientation between two topological map nodes [12]. Recent work on localization in pipe networks also incorporates both metric and topological information [13], and similar methods have been applied to autonomous road vehicles [14] [15] [16] [17].

The work presented in this paper presents an incorporation of measurement of distance into the localization method, and improvements to the accuracy and efficiency of the method from previous work [18]. Simulation on a large realistic network of pipes has been used to compare the proposed methods with a typical topological localization method. The effect of four uncertainty parameters on the

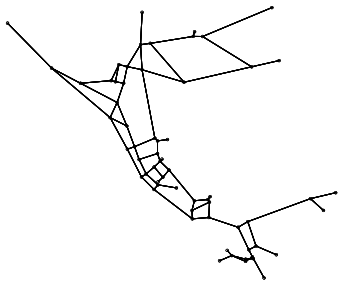

Fig. 1. The example simulated network of pipes used in this work, consisting of 63 nodes, which represent junctions, each connected to 1, 3, or 4 other nodes.

localization accuracy is measured, and the accuracy and efficiency is measured for the proposed methods.

2 Methods

2.1 State Definition

The robot moves in a network of pipes, shown in Fig. 1. The full robot state is defined as $s_{x_t x_{t-1} \theta_t} = [x_t,\ x_{t-1},\ \theta_t]$ and is composed of three components, facilitating localization of the robot [18]. The first component is the robot's discrete position, which is the junction index x at time index t. The second is the robot's discrete direction θ_t which is the index of the pipe which is has arrived from, allowing information about the robot's choice of action to be used in localization. The third is the robot's previous position x_{t-1}, allowing information about the length of the journey between junctions to be used in localization. The robot state is only updated at junctions or at ends of pipes, and the robot's position and orientation are not considered in transitions between these states.

The robot's belief in the state is represented as a vector $\boldsymbol{b}(\boldsymbol{s}_{x_t x_{t-1} \theta_t})$ over all possible values of the state, where each value is the estimated likelihood of being in that particular state. For the full state definition, there are $X^2 D$ possible states, where X is the number of nodes in the network and D is the maximum number of connections between nodes. The size of this vector is not a problem for small networks, however for the network in Fig. 1 there are 63 nodes and a maximum of 4 connection giving 15876 possible values of the state. The computational requirement for a vector this size is expected to be infeasible for the small robot required in this application, therefore alternatives to this state definition are proposed here.

The first improvement proposed is partial robot state definitions which reduce the size of the belief vector. The state definition $s_{x_t \theta_t}$ includes only the current position and direction of the robot. Measurements of the length of the journey between junctions can therefore not be incorporated exactly, however an approximation can be made which is described in section 2.4. The state definition s_{x_t} includes only the current position of the robot. The choice of action

can not be incorporated exactly, and an approximate means of doing this is not presented in this work.

The second improvement proposed is to truncate the belief vector at each step, and compute the updated belief only for states that have a predicted likelihood over a threshold, using only information relating to states that have a likelihood over another threshold. The belief in other states is set to a small default value. This is similar to previous implementations [10].

2.2 Robot Model

At a junction, the robot chooses a direction at random, relative to its own unknown orientation. In practice, this action would be chosen to best inspect the network, however this would not affect the localization result so is neglected here. There are four sources of uncertainty in the robot motion. Three of these are discrete uncertainties: There is a chance that the robot incorrectly executes the action and moves in a different direction [10]. Between junctions there is a chance that the robot is turned around and returns to the previous junction. When arriving at a junction there is a chance that the robot does not detect it, and continues moving in a random unknown direction, without updating the state estimate [11]. This model is illustrated as a discrete probability distribution shown in Fig. 2(a). The robot is modelled as moving at a constant velocity with multiplicative Gaussian noise, which is the fourth source of uncertainty.

It is assumed that the robot can make two kinds of observation. Firstly, it can detect the number of exits from a junction, which could be done using a camera, sonar, or a number of other sensing modes. For a robot which is able to control its motion, this measurement is assumed to be accurate as it would be able to hold position to confirm the observation. However in the case where a robot is moved with the flow in the pipe this assumption may be violated. Secondly, it can estimate the distance travelled since its last state update. This could be done using odometry or dead reckoning. To model the distance travelled in the case where a robot is turned around in a pipe and returns to the previous junction, a uniform probability distribution over twice the length of the pipe is used. These observations could be removed, changed, or added to without affecting the localization method. For example, use of an inertial measurement unit (IMU) might be useful for estimating the direction.

2.3 Localization Model

For the transition model between states, written as T, the localization model parameters used are set approximately to the values in the robot model described previously, as shown in Fig. 2(a), so that the robot does not have exact knowledge of the true motion model. An alternative model is also proposed, referred to as $\bar{T}$, where the transition probabilities are distributed more evenly. In this work the extreme case of a uniform distribution is used.

For the measurement model, written as M, the probability of making a given continuous measurement must be found. For a given state transition with a

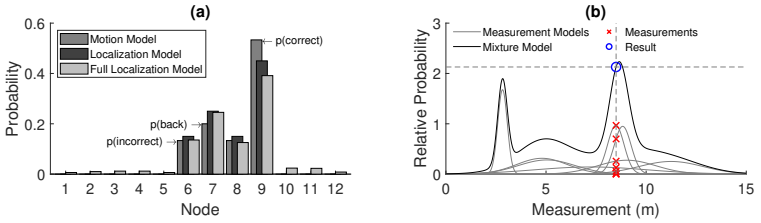

Fig. 2. (a) An example of the probability distribution for robot motion, in this case from node 2 in a 12 node network, showing the motion model used to simulate the robot motion, the estimate of this distribution used for localization, and the full localization model considering the probability of missing a node. (b) An example continuous probability distribution over possible measurements of distance between a pair of nodes.

number of possible transition lengths, the probability distribution over possible measurements is given by a sum of Gaussian distributions, illustrated in Fig. 2(b). A probability estimate is found as in equation 1 where $\tilde{p}$ is the relative probability estimate for measurement m given the possible state s', $K_{s'}$ is the number of Gaussian components, and $\sigma_{i,s'}$ and $\mu_{i,s'}$ are the standard deviation and mean for component i. The Gaussian model is relative and does not sum to one, as this would reduce the probabilities found for junction pairs with multiple short paths between them compared to junction pairs with single short paths where all the probability is concentrated around a single measurement.

$$\tilde{p}(m|s') = \sum_{i=1}^{K_{s'}} \frac{1}{\sigma_{i,s'}\sqrt{2\pi}} e^{-\frac{1}{2}\left(\frac{x-\mu_{i,s'}}{\sigma_{i,s'}}\right)} \tag{1}$$

As with the transition model, the parameters of the distribution used for localization are set to be different to those used to model the motion. In Fig. 2(b) the narrow Gaussian components represent simple transitions where the robot moves to a different junction. The wider Gaussian components model the added uniform distribution used to model the distance travelled when the robot returns to the junction it just left. For a single return incident this is not very accurate as the Gaussian distribution is a poor representation of the uniform distribution. However for multiple return incidents this is more accurate as the sum of multiple uniformly distributed variables is closer to the Gaussian distribution. This broad distribution should challenge the localization method, as a measurement is more likely to be seen as a good match for any given transition.

2.4 State Estimation

The forward algorithm is used to compute the discrete probability distribution, or belief, over the possible robot states in the Hidden Markov Model (HMM). With the state $s = s_{x_t x_{t-1} \theta_t}$, the typical form in Equation 2 is used to compute the updated belief $\boldsymbol{b'}$ over a vector of all possible new states $\boldsymbol{s'}$, based on the

belief $\boldsymbol{b}$ over a vector of possible states $\boldsymbol{s}$, the observation at the new position o, observation between positions m, action a, and transition and observation models T and P, decomposed into O and M. As the robot's previous position is used, this is similar to a second order HMM.

$$\boldsymbol{b}'(\boldsymbol{s}') = P(m, o|\boldsymbol{s}')T(\boldsymbol{s}'|\boldsymbol{s}, a)\boldsymbol{b}(\boldsymbol{s}) = M(m|\boldsymbol{s}')O(o|\boldsymbol{s}')T(\boldsymbol{s}'|\boldsymbol{s}, a)\boldsymbol{b}(\boldsymbol{s}) \tag{2}$$

When the state is $s = s_{x_t\theta_t}$, a modified form shown in Equation 3 is used to approximately incorporate information when measurements of distance between positions do not fit the typical form. A further modified form is used where the state is $s = s_{x_t}$, shown in Equation 4.

$$\boldsymbol{b}'(\boldsymbol{s}') = H(m|\boldsymbol{s}', \boldsymbol{b}(\boldsymbol{s}))O(o|\boldsymbol{s}')T(\boldsymbol{s}'|\boldsymbol{s}, a)\boldsymbol{b}(\boldsymbol{s}) \tag{3}$$

$$\boldsymbol{b}'(\boldsymbol{s}') = H(m|\boldsymbol{s}', \boldsymbol{b}(\boldsymbol{s}))O(o|\boldsymbol{s}')T(\boldsymbol{s}'|\boldsymbol{s})\boldsymbol{b}(\boldsymbol{s}) \tag{4}$$

where H is a diagonal matrix with each element given by Equation 5.

$$H(m|s', \boldsymbol{b}(\boldsymbol{s}))_{s'} = \boldsymbol{g}(m|s')\boldsymbol{b}(\boldsymbol{s}) \tag{5}$$

In these equations M is a diagonal matrix where each element is computed as in equation 1, and the vector $\boldsymbol{g}$ is the probability of measuring m for a transition to state s' from each state s and is computed similarly. The observation model O is similarly a diagonal matrix where each element is equal to one where the observation of number of exits from the junction matches the expected observation for the corresponding state. The transition model T is computed as described in section 2.3.

Where the robot's position is to be estimated, and the belief in each discrete position is distributed over a number of states corresponding to different directions and previous positions, some inference must be made. Summing the probabilities for all states for each discrete position and finding the largest value over positions does not necessarily give the same result as finding the largest probability over all states and finding the corresponding position. In this work the former method is used as it was observed to give a slightly better result.

Alternative algorithms such as the forward-backward algorithm or the Viterbi algorithm could be used instead of the forward algorithm. These would give better estimates of the full robot trajectory, at the cost of increased computation, which may be useful for path planning. The sensitivity to parameters and efficiency over each state and motion model definition are expected to be similar using these other algorithms, however this is not investigated in this work.

2.5 Practical Considerations

As the problem is considering only localization in a known environment, rather than mapping, the possible transition and measurement models can be precomputed for a given network [11].

For each junction for each direction, the transition model can be computed for each possible action, assuming that the connectivity between junctions is known.

When junctions can be missed, the state transition model is difficult to compute exactly. For a given network a Monte Carlo method is used to approximate the probability of transition between each state. The measurement model for distance travelled between junctions is also computed using the Monte Carlo method as all junction pairs have multiple possible paths between them. This is done assuming that the path length between junctions is known accurately. In this work using an idealised model network this is the case as all of the pipes are straight lines and the junction positions are known precisely. In practice there may be some uncertainty in these metric values, so a simultaneous localization and mapping approach may be required which uses the robot's measurements of distance travelled as well as prior information to find an accurate model.

3 Results

Experiments are done in simulation to compare the performance and computational requirements of localization using each of the proposed robot state definitions and improvements to efficiency. Aspects of the performance of the method in general can also be observed. An example of the result of the localization in the discrete space is shown in Fig. 3, where it is seen that the use of measured distance travelled improves the localization accuracy considerably.

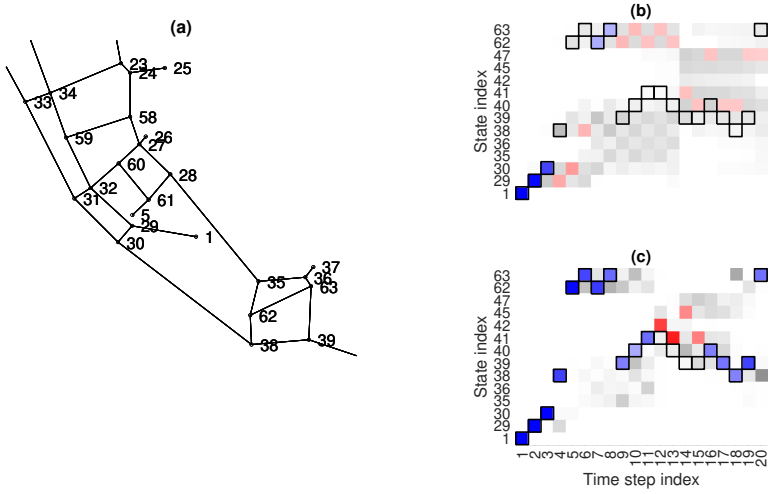

Fig. 3. An example of the localization method. (a) A subset of Fig. 1 showing the nodes labelled as state indices. (b, c) Part of the belief vector over each time step. The darkness corresponds to the belief for each state. The maximum belief at each step is labelled in blue if it is correct and red if it is incorrect. The true robot path through the states is shown by the bordered cells. (b) shows the result found without using the measured distance travelled, (c) shows the result using this measured distance.

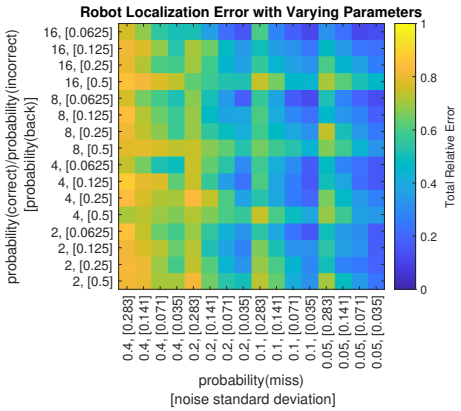

Fig. 4. Variation in localization error in a network with each combination of 4 values for each of the 4 uncertainty parameters: $p(correct)/p(incorrect)$, the relative probability of correctly executing an action, $p(back)$, the probability of returning to the previous node, $p(miss)$, the probability of missing a node, and the measurement noise amplitude. The total relative error is the proportion of the steps for which the localization is incorrect. The axes are labelled directly for each cell as the two quantities on each axis are varied to best visualise the four dimensional data.

3.1 Evaluation of Sensitivity to Model Parameters

The accuracy of the localization method is evaluated for different values for the uncertainty parameters described in section 2.2. The robot is simulated moving for 100 steps through the network shown in Fig. 1, and localization is done at each step. This is done ten times, starting from different points, and this is done for four different values for each of the four parameters.

For localization using the state definition $s_{x_t x_{t-1} \theta_t}$ the total relative error, the proportion of steps for which the localization estimate is incorrect, is shown for each of the 256 parameters sets in Fig. 4. Parameter sets which give low estimation error have low measurement noise, low probability of missing a junction and low probability of incorrectly returning to a junction. The relative probability of correctly executing an action is seen not to have much of an effect. It is expected that for a system with no uncertainty, the estimation error will be equal to zero, and that for a desired maximum error lower than that shown here, the required parameter values could be found by following the relationship to accuracy shown here.

These results are as expected. The probability of correctly executing an action affects only the discrete part of the model shown in Fig. 2(a), which is always quite accurate as the localization model in each case uses estimates of the parameter set. The other parameters have an effect on the measurement model shown in Fig. 2(b). The measurement noise directly affects the variance of the Gaussian components, so a larger magnitude of noise will increase the likelihood of an incorrect state appearing to be a good match for the measurement made.

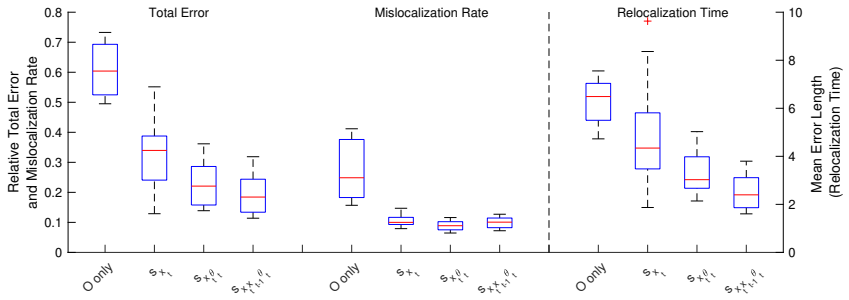

Fig. 5. A comparison of the results using each of the three state definitions (s_{x_t}, $s_{x_t\theta_t}$, $s_{x_t x_{t-1}\theta_t}$), and without using the measured distance m (O only). This is done for each of the three error metrics: *Total Error*, the proportion of steps for which the localization is incorrect, *Error Starts*, the proportion of steps where an initial mislocalization occurs, and the mean *Error Length*, the mean number of steps before relocalizing. The box plots show the quartiles for each value over a range of parameter sets determining the uncertainty in robot motion. The parameter values used are a subset of those shown in Fig. 4, using only the two values for each corresponding to the lower uncertainty.

The probability of moving back to the previous node increases the impact of the uniformly distributed measurements which are not modelled accurately in the localization model. The probability of missing a node increases the impact of the Gaussian components with higher mean values, which tend to be close together due to many longer paths existing with similar lengths. Therefore it is unsurprising that these parameters have an effect on the localization accuracy.

3.2 Comparison of Methods

Fig. 5 compares the results found using each state definition, over the subset of the parameter sets which correspond to the lower uncertainty, indicative of a good performance. The total error in localization is decomposed into two components: the number of steps at which an initial mislocalization occurs, and the mean number of steps before relocalization.

The median total error increases for the more reduced state definitions, largely due to the increase in mean number of steps before relocalizing after an error. Compared to only using observations at junctions, the use of measured distance travelled is seen to reduce the median localization error over the parameter sets by 66%, 62%, and 43% for each of the state definitions respectively, from least to most reduced. However, the results with the best set of parameters for each state definition are similar, giving around a 70% reduction in error.

Table 1 compares the median computation time per step for each of the state definitions in the exact and truncated methods, for two maps, one with 12 nodes and one with 63 nodes. Note that the exact values are expected to be different in practice on different hardware. The truncated method is shown to reduce the

Table 1. Median computation time τ with each state definition.

	Time s_{x_t} (s)		Time $s_{x_t\theta_t}$ (s)		Time $s_{x_t x_{t-1}\theta_t}$ (s)	
Network	Exact[a]	Truncated[b]	Exact	Truncated	Exact	Truncated
Map 1	0.003	0.002	0.007	0.003	0.016	0.007
Map 2	0.062	0.005	0.145	0.010	0.838	0.022

[a]Belief is computed for all possible states.
[b]Belief is computed for likely new states using likely states.

computation time significantly, especially for the larger map. Reducing the state definition is also shown to reduce the computation time substantially.

With a measure of computation time for each set of parameters, a measure of localization efficiency can be found for each method, given by

$$\eta = (1 - \epsilon)/\tau \tag{6}$$

where ϵ is the total relative localization error (the proportion of steps at which the estimate is incorrect), $1 - \epsilon$ is the relative localization accuracy, and τ is the computation time. This is shown for four sets of parameters in Table 2. For each method it can be seen that the ratio of accuracy to computation time is higher for parameters that give higher accuracy, suggesting that a robot able to give low uncertainty would give an improved accuracy and a lower computational power requirement. It is also seen here that this efficiency ratio is better for the more reduced state methods, especially for higher accuracy parameters.

Finally, Fig. 6 compares the localization estimate when using the motion models T and $\bar{T}$ (described in section 2.3), done here for the state definition s_{x_t} over the range of parameter sets. It is seen that the localization error is generally lower when using $\bar{T}$, especially at lower probabilities of missing a junction and lower noise. This is seen to be due to a decrease in the relocalization time, which compensates for a generally increased rate of mislocalization.

Over all of these comparisons between state definitions, the results found using the reduced state definition s_{x_t} are more efficient than those found with more full state definitions. This result is improved by using an alternative motion model $\bar{T}$, which is initially a surprising result, as this method is unable to incorporate information about the choice of action into the estimation. From this, it is suggested that the use of measured distance and observed number of exits at a junction are more important for successful localization than the motion model.

Table 2. Ratio (η) of accuracy ($1 - \epsilon$) to time taken (τ) for four sets of parameters.

	s_{x_t}		$s_{x_t\theta_t}$		$s_{x_t x_{t-1}\theta_t}$	
Parameters[a]	Accuracy	Ratio	Accuracy	Ratio	Accuracy	Ratio
[8,0.5,0.4,0.005]	0.2	10	0.19	15	0.23	4.7
[8,0.125,0.2,0.005]	0.37	40	0.58	51	0.62	18
[16,0.25,0.1,0.0013]	0.65	170	0.63	64	0.67	23
[16,0.0625,0.05,0.0013]	0.87	310	0.85	100	0.86	45

[a]The parameters are: probability(correct)/probability(incorrect), probability(back), probability(miss), measurement noise.

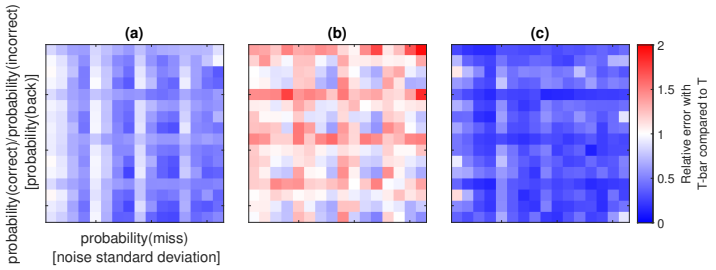

Fig. 6. A comparison between the results found using the models T and $\bar{T}$ with the state definition s_{x_t}, over the range of parameter sets. (a) shows the relative total error, (b) shows the relative mislocalization error, which is the proportion of initial incorrect estimates, and (c) shows the relative relocalization time, which is the mean number of steps before the estimate becomes correct. The value in each cell is equal to the result found using the $\bar{T}$ model divided by that using the T model. The axes are not labelled for conciseness, however they are identical to those found in Fig. 4.

It is speculated that the $\bar{T}$ model localization has an improved result as it keeps a more diverse belief across the possible states, so mislocalization is more likely but it is able to recover from error more quickly when a good measurement is made. This will be investigated in future work.

4 Conclusions and Further Work

Simulated results for topological robot localization in a network of pipes have been presented. The effect of four uncertainty parameters on the accuracy has been investigated and results are as would be expected. Parameter values required for good performance in this model are identified.

To improve on identified problems with complexity, two alternative state definitions have been developed and compared to the typical HMM-based method. It is seen more efficient performance is found using a reduced definition of robot state and an augmented HMM. An alternative motion model is also proposed which shows an improvement in accuracy. Future work will investigate this alternate method in more detail, and compare the methods in other network topologies. Further work could extend this method to a multi-robot case.

References

1. P. Hansen, H. Alismail, P. Rander, and B. Browning, "Pipe mapping with monocular fisheye imagery," *IEEE International Conference on Intelligent Robots and Systems*, pp. 5180–5185, 2013.
2. A. C. Murtra and J. M. Mirats Tur, "IMU and cable encoder data fusion for in-pipe mobile robot localization," *IEEE Conference on Technologies for Practical Robot Applications, TePRA*, pp. 1–6, 2013.

3. Y. Bando, H. Suhara, M. Tanaka, T. Kamegawa, K. Itoyama, K. Yoshii, F. Matsuno, and H. G. Okuno, "Sound-based online localization for an in-pipe snake robot," *SSRR 2016 - International Symposium on Safety, Security and Rescue Robotics*, pp. 207–213, 2016.
4. K. Ma, M. M. Schirru, A. H. Zahraee, R. Dwyer-Joyce, J. Boxall, T. J. Dodd, R. Collins, and S. R. Anderson, "Robot mapping and localisation in metal water pipes using hydrophone induced vibration and map alignment by dynamic time warping," *Proceedings - IEEE International Conference on Robotics and Automation*, pp. 2548–2553, 2017.
5. B. Kuipers and Y. T. Byun, "A robot exploration and mapping strategy based on a semantic hierarchy of spatial representations," *Robotics and Autonomous Systems*, vol. 8, no. 1-2, pp. 47–63, 1991.
6. D. Kortenkamp and T. Weymouth, "Topological mapping for mobile robots using a combination of sonar and vision sensing," *Proceedings of the National Conference on Artificial Intelligence*, vol. 2, pp. 979–984, 1994.
7. S. Thrun, "Learning metric-topological maps for indoor mobile robot navigation," *Artificial Intelligence*, vol. 99, no. 1, pp. 21–71, 1998.
8. H. Choset and K. Nagatani, "Topological simultaneous localization and mapping (SLAM): towardexact localization without explicit localization," *IEEE Transactions on Robotics and Automation*, vol. 17, no. 2, pp. 125–137, 2001.
9. A. R. Cassandra, L. P. Kaelbling, and J. A. Kurien, "Acting under uncertainty: discrete Bayesian models for mobile-robot navigation," *IEEE International Conference on Intelligent Robots and Systems*, vol. 2, no. May, pp. 963–972, 1996.
10. J. Hertzberg and F. Kirchner, "Landmark-based autonomous navigation in sewerage pipes," *Proceedings of the 1st Euromicro Workshop on Advanced Mobile Robots, EUROBOT 1996*, pp. 68–73, 1996.
11. C. Gomez, A. C. Hernandez, J. Crespo, and R. Barber, "Uncertainty-based localization in a topological robot navigation system," *2017 IEEE International Conference on Autonomous Robot Systems and Competitions, ICARSC 2017*, pp. 67–72, 2017.
12. C. Gomez, A. C. Hernandez, L. Moreno, and R. Barber, "Qualitative Geometrical Uncertainty in a Topological Robot Localization System," *Proceedings - 2018 International Conference on Control, Artificial Intelligence, Robotics and Optimization, ICCAIRO 2018*, pp. 183–188, 2018.
13. D. Alejo, F. Caballero, and L. Merino, "A robust localization system for inspection robots in sewer networks," *Sensors (Switzerland)*, vol. 19, no. 22, pp. 1–28, 2019.
14. M. E. El Najjar and P. Bonnifait, "A Road-Matching Method for Precise Vehicle Localization Using Belief Theory and Kalman Filtering," *Autonomous Robots 19, 173–191, 2005*, pp. 173–191, 2005.
15. M. A. Brubaker, A. Geiger, and R. Urtasun, "Map-Based Probabilistic Visual Self-Localization," *IEEE Transactions on Pattern Analysis and Machine Intelligence*, vol. 38, no. 4, pp. 652–665, 2016.
16. F. Bernuy and J. Ruiz-del Solar, "Topological Semantic Mapping and Localization in Urban Road Scenarios," *Journal of Intelligent and Robotic Systems: Theory and Applications*, vol. 92, no. 1, pp. 19–32, 2018.
17. C. Fouque, P. Bonnifait, D. Bétaille, and A. Working, "Enhancement of Global Vehicle Localization using Navigable Road Maps and Dead-Reckoning," *2008 IEEE/ION Position, Location and Navigation Symposium*, pp. 1286–1291, 2008.
18. R. Worley and S. Anderson, "Topological Robot Localization in a Pipe Network," *UKRAS20 Conference: "Robots into the real world" Proceedings*, pp. 59–60, 2020.